Implementation of the foil-on-hohlraum technique for the magnetic recoil spectrometer for time-resolved neutron measurements at the National Ignition Facility

C. E. Parker, J. A. Frenje, M. Gatu Johnson, D. J. Schlossberg, H. G. Reynolds, L. Berzak Hopkins, R. Bionta, D. T. Casey, S. J. Felker, T. J. Hilsabeck, J. D. Kilkenny, C. K. Li, A. J. Mackinnon, H. Robey, M. E. Schoff, F. H. Séguin, C. W. Wink, and R. D. Petrasso

Citation: Review of Scientific Instruments **89**, 113508 (2018); doi: 10.1063/1.5052184
View online: https://doi.org/10.1063/1.5052184
View Table of Contents: http://aip.scitation.org/toc/rsi/89/11
Published by the American Institute of Physics

Implementation of the foil-on-hohlraum technique for the magnetic recoil spectrometer for time-resolved neutron measurements at the National Ignition Facility

C. E. Parker,[1,a)] J. A. Frenje,[1] M. Gatu Johnson,[1] D. J. Schlossberg,[2] H. G. Reynolds,[3] L. Berzak Hopkins,[2] R. Bionta,[2] D. T. Casey,[2] S. J. Felker,[2] T. J. Hilsabeck,[3] J. D. Kilkenny,[3] C. K. Li,[1] A. J. Mackinnon,[2] H. Robey,[2] M. E. Schoff,[3] F. H. Séguin,[1] C. W. Wink,[1] and R. D. Petrasso[1]
[1]*Massachusetts Institute of Technology, Cambridge, Massachusetts 02139, USA*
[2]*Lawrence Livermore National Laboratory, Livermore, California 94550, USA*
[3]*General Atomics, San Diego, California 92186, USA*

(Received 14 August 2018; accepted 2 November 2018; published online 20 November 2018)

The next-generation Magnetic Recoil Spectrometer, called MRSt, will provide time-resolved measurements of the deuterium-tritium-neutron spectrum from inertial confinement fusion implosions at the National Ignition Facility. These measurements will provide critical information about the time evolution of the fuel assembly, hot-spot formation, and nuclear burn. The absolute neutron spectrum in the energy range of 12-16 MeV will be measured with high accuracy (~5%), unprecedented energy resolution (~100 keV) and, for the first time ever, time resolution (~20 ps). Crucial to the design of the system is a CD conversion foil for the production of recoil deuterons positioned as close to the implosion as possible. The foil-on-hohlraum technique has been demonstrated by placing a 1-mm-diameter, 40-μm-thick CD foil on the hohlraum diagnostic band along the line-of-sight of the current time-integrated MRS system, which measured the recoil deuterons. In addition to providing validation of the foil-on-hohlraum technique for the MRSt design, substantial improvement of the MRS energy resolution has been demonstrated. *Published by AIP Publishing.* https://doi.org/10.1063/1.5052184

I. INTRODUCTION AND MOTIVATION

Time-integrated diagnostics, such as neutron time-of-flight (nTOF) spectrometers[1,2] and the Magnetic Recoil Spectrometer (MRS),[3–5] have routinely measured the yield, down-scatter ratio (DSR), and ion temperature (T_{ion}) in deuterium-tritium (DT) implosions at the National Ignition Facility (NIF).[6] These diagnostics are crucial to the facility; however, in order to assess how the fuel assembly and nuclear burn evolve during the implosion, time-resolved neutron measurements are the key. The MRSt[7–9] is being designed as the first instrument for time-resolved measurements of these parameters.

The current MRSt design consists of the following main components: a thin CD foil, positioned on the hohlraum about 4 mm from target chamber center (TCC), which generates recoil deuterons; four electromagnets, two quadrupoles and two dipoles, to focus the recoil deuterons; a CsI photocathode positioned at the focal plane for detection of ions and secondary electron (SE) production; a pulse-dilation drift tube for un-skewing and dilating the SE; a microchannel plate and segmented anode array at the end of the drift tube; and shielding for neutrons and γ-rays enclosing the pulse-dilation drift tube. The aspects of the design that are fixed are the magnet design, the use of the foil attached to the hohlraum, and selecting lead-free microchannel plates for the SE gain. The foils for the final design will be selected from a pre-determined list, approximately 400 μm in diameter with varying CD thicknesses, to help balance statistics and energy resolution based upon the expected DT neutron yields.

A key component of the MRSt design is the CD conversion foil used to produce recoil deuterons, scattered by DT neutrons, which are momentum-analyzed by a multiple-magnet system before being detected by a focal plane detector. The current time-integrating MRS systems[10] at both OMEGA[11] and the NIF use large, well-characterized, CD foils placed at a known distance from TCC. These configurations are sufficient for time-integrated measurements; however, in order to preserve the timing information desired for the MRSt, the ion-optics design requires nearly a point source of recoil deuterons. To accommodate such a requirement, the conversion foil needs to be placed as close as possible to TCC and therefore the neutron source.

This paper discusses the technique developed to field thin CD foils mounted on the outside of the hohlraum. Section II describes the foil fabrication and placement on the diagnostic band of the hohlraum. Section III discusses tests of the concept on three facility diagnostic shots and the measured results using the currently implemented MRS. Finally, Sec. IV describes the implications for the path forward for the MRSt and MRS based on these results.

II. FOIL CONSIDERATIONS

A. Foil fabrication and characterization

Two different types of tantalum-backed CD foils were fabricated by General Atomics for this proof-of-principle study

a)Author to whom correspondence should be addressed: cparker@psfc.mit.edu.

using similar techniques developed for the current MRS system,[12] with a 1-mm diameter chosen to ensure that there would be sufficient statistics for the measurement. Both foil types were glow-discharge polymer (GDP) CD coated onto nominally 45-μm-thick, 1-mm-diameter polished tantalum backing. The characteristics of the CD foil are a density of 1.1 ± 0.1 g/cc and a D:C ratio of 1.46 ± 0.05. The foil types delivered for the shots were flat or bent with a radius of curvature to match that of the diagnostic band of the thermo-mechanical package (TMP). To be certain that the foil was placed in the appropriate orientation, with the Ta backing facing TCC, it was determined that curved foils would be best to mitigate failure. A visible inspection as to whether or not the foil had "wings" if attempted to be placed incorrectly could be conducted during the assembly process.

To fabricate the foils, the first step was to polish the Ta substrate to be used as the backing material. This bulk material was polished to a thickness of 45 μm, with the characterized roughness on average being 0.2 μm. From this bulk material, two procedures were attempted for producing the 1-mm-diameter coated foils. The first attempt was to GDP coat the entire bulk and then to laser cut the individual foils. For the second attempt, 1-mm-diameter disks were laser cut with a small tab to hold them in the bulk, then GDP coated, then gently removed from the bulk material.

As GDP can potentially de-laminate from the substrate, particularly while laser cutting, attempting both provided insight into which would be more successful for the test foils as well as the future routine foils. In addition to the concern of de-laminating, the possibility was present that sharp edges on the cut tantalum backing could potentially damage other delicate parts of the assembly, therefore ruining the hohlraum build. Coating on the edges of the Ta backing would be more probable for foils that were cut then coated, which would cause issues with the produced signal as it would be difficult to account for in the instrument response function (IRF) calculations.

For the foils that were coated and then laser cut, the CD de-laminated from the Ta backing, and thus could not be further characterized or curved to match the TMP. The laser cut and then coated foils were successfully removed from the bulk material with minimal CD coating on the edges. Upon this success, the curved foils were attempted by beginning with polished bulk Ta that was bent around a metal dowel. The 1-mm-diameter foils were cut and held in the bulk with tabs, CD coated, and then removed. Different diameters of the initial curve were added to the bulk as the final curve of the foil would change due to the spring back of the metal caused by the addition of the GDP. To add the requested curvature of ~4-mm radius to the foil, the best results were from beginning with 2-mm-radius curved Ta.

Both the flat and curved foils were characterized in terms of surface roughness and thickness with five-point measurements of the GDP coating. This information is essential to the MRSt IRF calculation. For the flat foils, the surface roughnesses ranged from 1.01 to 1.50 μm root-mean-square roughness (Rq), while for the curved foils, the surface roughness ranged from 1.32 to 1.82 μm Rq. This was unexpected, but likely due to the higher-than-usual rate at which the GDP was coated onto the Ta backing. The curved foils with the three lowest values for roughness were chosen for the target builds as the curvature would help mitigate failure due to the visible correct orientation of the foil with respect to the TMP.

B. Foil placement on the hohlraum

To measure the recoil deuterons from the CD foil, the MRS was used. The dimensions of the CD foils would allow for a balance between energy resolutions of the system while not sacrificing measurement efficiency. The system can be configured to measure both recoil protons and deuterons, depending on the number of CR-39 detectors selected and the filtering thickness and type placed in front of them, allowing for more customizable setups. In addition, the IRF can be independently calculated from the first principles for the as-built configuration.

As the MRS is positioned along the line-of-sight (LOS) with a polar angle of 73° and an azimuthal angle of 324°, the foils were positioned on the hohlraum along this LOS. Figure 1 shows the nominal placement of the foil on the TMP (given in spherical chamber coordinates). The diagnostic band included a Mylar window used by other diagnostics. This Mylar window is nominally 6-μm thick and 13.1 mm^2 in area. A batch of CH foils for these tests, to attempt to measure recoil protons, was not manufactured due to concern for potential signal contamination from the protons originating from the Mylar window.

C. Impact of heating and scattered laser light on foil

Due to the fragile nature of the CD foils and the close proximity to TCC, understanding the potential impacts of heating and unconverted laser light on the characteristics of the foil was an important aspect of this proof-of-principle study. This prompted a VISRAD[13] evaluation of the surrounding conditions and their impact on the CD foil. Figure 2 shows the radiation temperature, T_r, during the main laser pulse for a similar peak laser power to the pulse requested for the foil-on-hohlraum test shots.

With a mass ablation rate (g/cm^2/s) for a given material of $\dot{m} = 3 \times 10^5 T_r^3$, where T_r is in hundredths of eV,[14] a temperature of 26 eV, as determined from the VISRAD, will ablate 5273 g/cm^2/s. For the calculation, the bang time for a

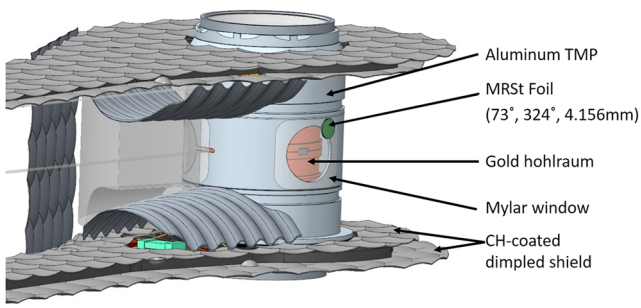

FIG. 1. Nominal placement of the 1-mm-diameter CD foil on the diagnostic band in spherical target chamber coordinates.

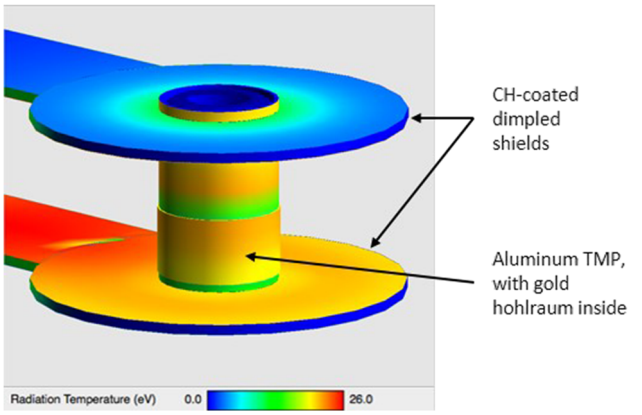

FIG. 2. VISRAD model of the target, which includes the aluminum TMP, gold hohlraum (inside the TMP), and CH-coated dimpled shields, during the main laser pulse. The radiation temperature in the external hohlraum is ~26 eV throughout the main drive of the laser pulse. Additionally, based on the VISRAD, the unconverted laser power primarily hits the outer surfaces of the shields and does not directly illuminate the TMP.

companion shot with the same requested laser pulse was ~7 ns. Therefore over the duration of the exposure to the radiation field, 3.7×10^{-2} mg/cm^2, or 0.34 μm of CD material will be ablated from the surface. This corresponds to ~0.8% of the material, which is negligible for the efficiency and response calculations.

III. FOIL-ON-HOHLRAUM TESTS

The foil-on-hohlraum configuration was fielded on three facility diagnostic shots: N171022-002, N171112-002, and N171120-001.[15] This series was chosen as it was designed for neutron diagnostic calibrations with expected DT yields of approximately 10^{15}. The capsule with a high-density carbon ablator would also have insignificant impact on the MRS signal as there would not be CD in the shell material to produce elastically scattered deuterons.

Figure 3 shows the CD foil placed on the TMP as well as a zoom-in of the CD foil itself. The technique used to place the foil was based upon previous work in gluing samples along the TMP for use in radiochemistry experiments.[16] The position tolerance for the foil placement is ±50 μm in both the dispersive and non-dispersive directions of the MRS system. This corresponds to ±0.7° for the nominal radial placement of 4.156 mm from TCC. This value was limited by uncertainty in the physical placement of the foil during the target build and the uncertainty in the alignment of the target within the NIF chamber.[17]

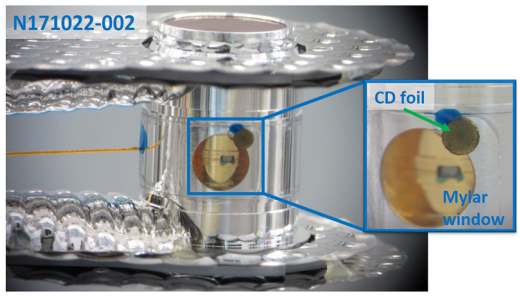

FIG. 3. Side-on photograph of the target build for shot N171022-002. The inset is a zoomed-in photograph of the CD foil, with the Mylar diagnostic window visible behind. The rough surfaces visible on the foil are real features, as described in Sec. II A. IM: LLNL-PHOTO-739929.

This uncertainty in placement for the 1-mm-diameter foils corresponds to ±0.2 keV in T_{ion} measurements and was determined by moving the foil in the simulation and seeing what the ±50 μm displacement corresponded to in terms of impact on broadening. The primary impact of foil misplacement is an increase in the average scattering angle. As the recoil deuteron energy is proportional to $E_n \cos(\theta)^2$, where E_n is the neutron energy in MeV and θ is the scattering angle, small angular changes at larger scattering angle have a bigger impact than at smaller scattering angle. The foil misplacement uncertainty is the biggest source of uncertainty on T_{ion} in this configuration. If the foil location is known perfectly, other sources of uncertainty, e.g., foil thickness, density, distance from TCC, radius, magnet aperture size, and distance together only give a ±0.13 keV systematic uncertainty in T_{ion}, therefore, achieving high precision in the foil placement for each shot is important.

Table I summarizes the positions of each foil in target chamber coordinates. The desired placement uncertainty was achieved for the first two target builds; however, on the third build, the foil was misaligned by approximately 70 μm in the non-dispersive direction and 330 μm in the dispersive direction. This could not be adjusted prior to the shot due to the risk of damaging the Mylar window and TMP glue joints. However, this provided for an excellent opportunity to study tolerances in the foil positioning and the impact on the yield and T_{ion} measurements.

A. Results

Figure 4 shows MRS data for shot N171022-002. The dispersive and non-dispersive directions of the magnet correspond to X and Y, respectively. The deuteron signal is concentrated in a vertical band to the left of the processed

TABLE I. Foil thickness, area, roughness, and location in spherical chamber coordinates for each of the three foil-on-hohlraum target builds. The average thickness of the polished Ta backing for each foil was 44 ± 1 μm. The second foil was placed the closest to specification of the three.

Shot number	CD thickness (μm)	CD area (mm^2)	Roughness (μm)	Location
N171022-002	39 ± 1	3.14 ± 0.20	1.320	73.76°, 324.275°, 4.173 mm
N171112-002	41 ± 1	3.14 ± 0.20	1.339	73.17°, 324.32°, 4.188 mm
N171120-001	38 ± 1	3.20 ± 0.20	1.362	74.01°, 328.71°, 4.149 mm

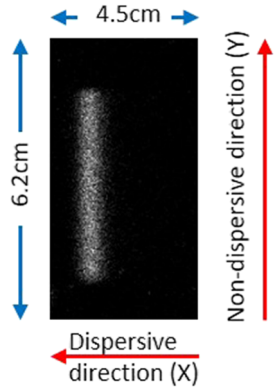

FIG. 4. MRS data for shot N171022-002. From this image, the MRS spectrum can be determined, from which the yield and T_{ion} can be determined.

image. Using the location-to-deuteron energy relationship, known from simulations, the location of the tracks along the CR-39 can be projected onto the dispersive axis to produce a histogram of the number of tracks per MeV. For more details on how MRS data are processed, the reader is referred to Refs. 10 and 18.

Figure 5 shows the MRS spectra for each shot. Fits for each shot include an IRF calculated for the specific foil placement and a flat CD foil with the correct thickness and area specifications. On the third shot, the offset of the foil along the dispersive direction visibly broadened the signal,

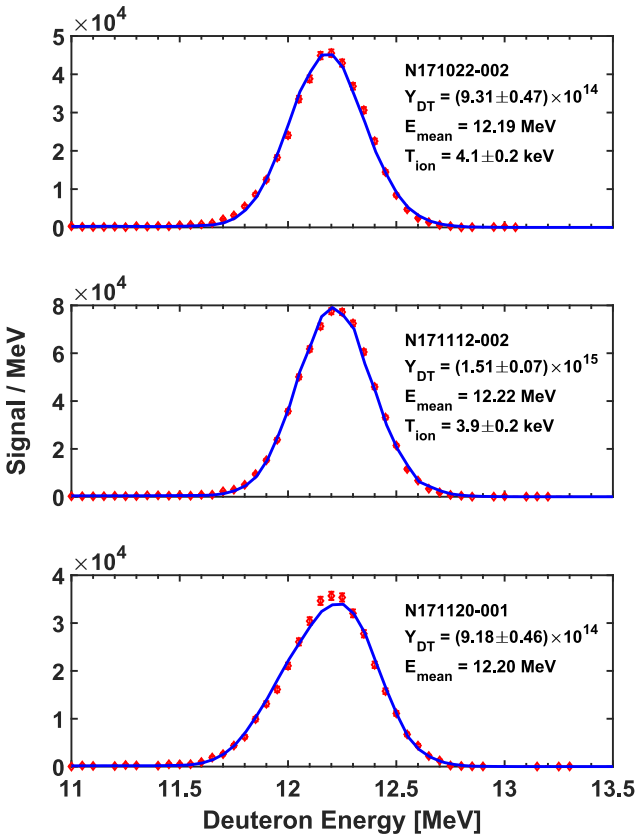

FIG. 5. Primary deuteron spectra for (top) N171022-002, (middle) N171112-002, and (bottom) N171120-001. The additional broadening of ~100 keV FWHM in the third shot is attributed to the foil being placed ~330 μm offset in the dispersive direction.

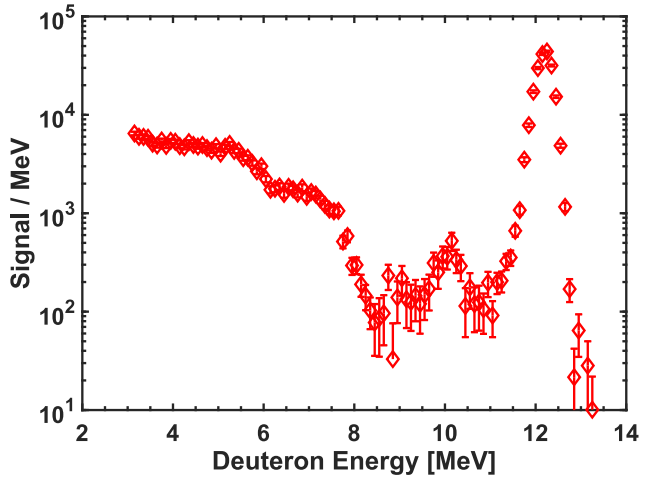

FIG. 6. The full MRS deuteron spectrum for shot N171022-002, which includes the undesired feature of a peak at ~10 MeV, due to CD material on the side of the Ta backing facing TCC. This undesired peak emphasizes the importance of eliminating CD on surfaces of the Ta that are not facing the MRS LOS. Note the primary peak at ~12 MeV.

especially compared with the nominally placed foil results. As the foil was curved to the TMP, but not entirely along the desired LOS, the scattering angle at which the recoil deuterons left the foil would not be the same as for the centered foil. An adjusted IRF was used to generate the fit for the third shot by translating the foil from the central position. However, additional work needs to be performed to fully account for offset foils in the future, particularly taking into account the curvature of the hohlraum as the foil is moved around it from the desired LOS. As the hohlraum radius of curvature is ~0.42 cm that means that a 300-μm offset along the hohlraum wall will effectively "tilt" the foil ~4° in the MRS LOS, leading to a different effective foil thickness. Additional improvement could possibly be made by incorporating the curvature of the foil itself.

For shot N171022-002, the MRS was configured to measure deuterons in the energy range of 3–15 MeV. This was

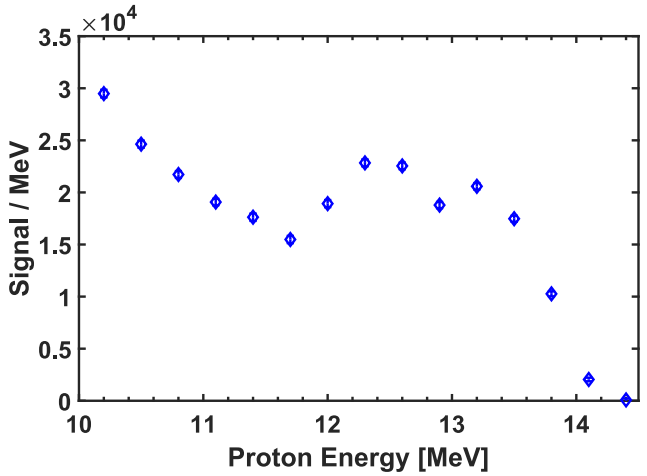

FIG. 7. The proton spectrum measured on shot N171112-002. The background of protons from the Mylar window and other nearby components, particularly at higher energies, could adversely impact MRSt measurements if using CH foils.

TABLE II. The DT yields and T_{ion} inferred from the MRS and nTOF data; the nTOF values listed are the average of several nTOF measurements. The MRS yield uncertainties include the contribution from both statistical and systematic sources. The T_{ion} is not reported for MRS on the third shot due to the foil misplacement causing a large uncertainty.

	Primary DT yield		T_{ion} (keV)	
Shot number	MRS	nTOFs	MRS	nTOFs
N171022-002	$(9.31 \pm 0.47)\times10^{14}$	$(9.01 \pm 0.28)\times10^{14}$	4.1 ± 0.2	4.27 ± 0.18
N171112-002	$(1.51 \pm 0.07)\times10^{15}$	$(1.58 \pm 0.05)\times10^{15}$	3.9 ± 0.2	4.08 ± 0.12
N171120-001	$(9.18 \pm 0.46)\times10^{14}$	$(9.49 \pm 0.29)\times10^{14}$	...	4.24 ± 0.20

performed to check for lower-energy contributions in the spectrum that could negatively impact using this configuration as a DSR measurement. Figure 6 shows the results of this measurement. The signal that peaks at approximately 10 MeV corresponds in energy to recoil deuterons from the primary neutrons that have traversed through ~40 μm of Ta. This indicates that some small amount of CD could have been on the frontside (facing TCC) of the nominally 45-μm-thick Ta backing. In addition, the signal below ~8 MeV is believed to be from the knock-on deuterons[19] from the implosion ranging through material thicknesses along the MRS LOS.

For shot N171112-002, a MRS configuration that was set up to measure protons in the energy range of 10–14 MeV to check for any background issues near the source, and the resulting spectrum is shown in Fig. 7. The structure between 12 and 14 MeV, which could adversely impact MRSt measurements if the system is re-configured to use CH foils, is due to a combination of the Mylar window and glue used to seal the Mylar window. The lower-energy contribution is likely from a combination of additional target build materials such as the 200-μm-thick aluminum diagnostic band, CH-coated dimpled shields, components of the TMP subassembly, the glue used in other parts of the target assembly, as well as deuteron breakup, which gives a proton continuum up to 11.8 MeV. Significant quantities of glue are needed around the edge of the Mylar window and along the TMP joints to create the vacuum-tight seal and are not easily quantifiable. The overall level of contribution of each background source material is currently being investigated.

Table II summarizes the DT yields and ion temperatures inferred from the MRS and nTOF data. The reduction in yield on the first and last shots is expected as these implosions were purposely driven with a strong laser-drive P1 asymmetry, therefore reducing the yields.[15] The apparent T_{ion}, as determined from the nTOFs and MRS, agrees within error bars for the first two shots. The MRS T_{ion} value for the third shot is not reported as there is ~1.3 keV uncertainty in the value due to the foil misplacement.

IV. PATH FORWARD AND CONCLUSION

The success of the foil-on-hohlraum proof-of-principle study provides guidance for the fabrication of the CD foils for the MRSt. To measure the DSR, it has been determined that a Ta backing greater than 45 μm is necessary in case there is CD on the frontside of the Ta backing. Due to the presence of a proton background from the Mylar window and the glue used to adhere it to the TMP, it has been determined that the best configuration for the MRSt will use a CD foil for recoil deuterons.

From the foil fabrication point of view, improvement in the GDP smoothness is essential for the physics shots, particularly for generating an accurate IRF for the T_{ion} measurements. As the roughness can lead to thickness variation, recoil deuterons could potentially range differently as they exit the foil, leading to a variation in response. This would negatively impact the shape of the primary peak, making it more difficult to study the physics from detailed shape measurements. In addition, the effort to pre-bend the foils before coating would not be necessary for the thicker Ta backing because that can be scratched with a fiducial marking on the back side to assist in the target assembly process. However, even with the thicker Ta, it is still undesirable to have CD on the frontside or edges of the Ta backing.

In addition to MRSt development, this concept can be used with the current NIF MRS system for higher resolution measurements at the same efficiency, even surpassing the results from the recent foil upgrade.[20] Smaller diameter foils with ~100-μm-thick Ta backing with different CD thicknesses, ranging from 2.5 μm to 40 μm, selected appropriately based on the expected DT neutron yield, could greatly improve the energy resolution of the measurements. Preliminary calculations indicate that an energy resolution of ~180 keV FWHM could be achieved for the primary DT neutron peak for a configuration using a 500-μm-diameter, 20-μm-thick CD foil. This is three times better resolution than the current MRS high-res mode. The success of this concept has also prompted exploring modification of the OMEGA MRS[21] to allow for a closer, smaller foil to provide an independent T_{ion} measurement on implosions of cryogenically layered targets.[22]

ACKNOWLEDGMENTS

The authors would like to thank Michelle Valadez for processing the CR-39 used in this work and the NIF operations crew for their efforts in operating the MRS in a non-standard configuration. This work was performed under the auspices of the U.S. Department of Energy by Lawrence Livermore National Laboratory under Contract No. DE-AC52-07NA27344. This report was prepared as an account of work

[1]T. J. Clancy, J. Caggiano, J. McNaney, M. Eckart, M. Moran, V. Y. Glebov, J. Knauer, R. Hatarik, S. Friedrich, R. Zacharias, A. Carpenter, M. J. Shoup, T. Buczek, M. Yeoman, Z. Zeid, N. Zaitseva, B. Talison, J. Worden, B. Rice, T. Duffy, A. Pruyne, and K. Marshall, Proc. SPIE **9211**, 92110A (2014).

[2]R. Hatarik, D. B. Sayre, J. A. Caggiano, T. Phillips, M. J. Eckart, E. J. Bond, C. Cerjan, G. P. Grim, E. P. Hartouni, J. P. Knauer, J. M. Mcnaney, and D. H. Munro, J. Appl. Phys. **118**, 184502 (2015).

[3]J. A. Frenje, D. T. Casey, C. K. Li, F. H. Séguin, R. D. Petrasso, V. Y. Glebov, P. B. Radha, T. C. Sangster, D. D. Meyerhofer, S. P. Hatchett, S. W. Haan, C. J. Cerjan, O. L. Landen, K. A. Fletcher, and R. J. Leeper, Phys. Plasmas **17**, 056311 (2010).

[4]M. G. Johnson, J. A. Frenje, D. T. Casey, C. K. Li, F. H. Séguin, R. Petrasso, R. Ashabranner, R. M. Bionta, D. L. Bleuel, E. J. Bond, J. A. Caggiano, A. Carpenter, C. J. Cerjan, T. J. Clancy, T. Doeppner, M. J. Eckart, M. J. Edwards, S. Friedrich, S. H. Glenzer, S. W. Haan, E. P. Hartouni, R. Hatarik, S. P. Hatchett, O. S. Jones, G. Kyrala, S. Le Pape, R. A. Lerche, O. L. Landen, T. Ma, A. J. MacKinnon, M. A. McKernan, M. J. Moran, E. Moses, D. H. Munro, J. McNaney, H. S. Park, J. Ralph, B. Remington, J. R. Rygg, S. M. Sepke, V. Smalyuk, B. Spears, P. T. Springer, C. B. Yeamans, M. Farrell, D. Jasion, J. D. Kilkenny, A. Nikroo, R. Paguio, J. P. Knauer, V. Y. Glebov, T. C. Sangster, R. Betti, C. Stoeckl, J. Magoon, M. J. Shoup, G. P. Grim, J. Kline, G. L. Morgan, T. J. Murphy, R. J. Leeper, C. L. Ruiz, G. W. Cooper, and A. J. Nelson, Rev. Sci. Instrum. **83**, 10D308 (2012).

[5]J. Frenje, R. Bionta, E. Bond, J. Caggiano, D. Casey, C. Cerjan, J. Edwards, M. Eckart, D. Fittinghoff, S. Friedrich, V. Glebov, S. Glenzer, G. Grim, S. Haan, R. Hatarik, S. Hatchett, M. G. Johnson, O. Jones, J. Kilkenny, J. Knauer, O. Landen, R. Leeper, S. L. Pape, R. Lerche, C. Li, A. Mackinnon, J. McNaney, F. Merrill, M. Moran, D. Munro, T. Murphy, R. Petrasso, R. Rygg, T. Sangster, F. Séguin, S. Sepke, B. Spears, P. Springer, C. Stoeckl, and D. Wilson, Nucl. Fusion **53**, 043014 (2013).

[6]G. H. Miller, E. I. Moses, and C. R. Wuest, Nucl. Fusion **44**, S228 (2004).

[7]J. A. Frenje, T. J. Hilsabeck, C. W. Wink, P. Bell, R. Bionta, C. Cerjan, M. G. Johnson, J. D. Kilkenny, C. K. Li, F. H. Séguin, and R. D. Petrasso, Rev. Sci. Instrum. **87**, 11D806 (2016).

[8]T. J. Hilsabeck, J. A. Frenje, J. D. Hares, and C. W. Wink, Rev. Sci. Instrum. **87**, 11D807 (2016).

[9]C. W. Wink, J. A. Frenje, T. J. Hilsabeck, R. Bionta, H. Y. Khater, M. G. Johnson, J. D. Kilkenny, C. K. Li, F. H. Séguin, and R. D. Petrasso, Rev. Sci. Instrum. **87**, 11D808 (2016).

[10]D. T. Casey, J. A. Frenje, M. G. Johnson, F. H. Séguin, C. K. Li, R. D. Petrasso, V. Y. Glebov, J. Katz, J. Magoon, D. D. Meyerhofer, T. C. Sangster, M. Shoup, J. Ulreich, R. C. Ashabranner, R. M. Bionta, A. C. Carpenter, B. Felker, H. Y. Khater, S. LePape, A. MacKinnon, M. A. McKernan, M. Moran, J. R. Rygg, M. F. Yeoman, R. Zacharias, R. J. Leeper, K. Fletcher, M. Farrell, D. Jasion, J. Kilkenny, and R. Paguio, Rev. Sci. Instrum. **84**, 043506 (2013).

[11]T. Boehly, D. Brown, R. Craxton, R. Keck, J. Knauer, J. Kelly, T. Kessler, S. Kumpan, S. Loucks, S. Letzring, F. Marshall, R. McCrory, S. Morse, W. Seka, J. Soures, and C. Verdon, Opt. Commun. **133**, 495 (1997).

[12]H. G. Reynolds, M. E. Schoff, M. P. Farrell, M. G. Johnson, R. M. Bionta, and J. A. Frenje, Fusion Sci. Technol. **70**, 365 (2016).

[13]J. MacFarlane, J. Quant. Spectrosc. Radiat. Transfer **81**, 287 (2003).

[14]J. D. Lindl, *Inertial Confinement Fusion: The Quest for Ignition and Energy Gain Using Indirect Drive* (Springer-Verlag, New York, 1998).

[15]D. Schlossberg *et al.* (unpublished).

[16]D. A. Shaughnessy, N. Gharibyan, K. J. Moody, J. D. Despotopulos, P. M. Grant, C. B. Yeamans, L. B. Hopkins, C. J. Cerjan, D. H. G. Schneider, and S. Faye, J. Phys.: Conf. Ser. **717**, 012080 (2016).

[17]E. T. Alger, J. Kroll, E. G. Dzenitis, R. Montesanti, J. Hughes, M. Swisher, J. Taylor, K. Segraves, D. M. Lord, J. Reynolds, C. Castro, and G. Edwards, Fusion Sci. Technol. **59**, 78 (2011).

[18]D. T. Casey, J. A. Frenje, F. H. Séguin, C. K. Li, M. J. Rosenberg, H. Rinderknecht, M. J.-E. Manuel, M. G. Johnson, J. C. Schaeffer, R. Frankel, N. Sinenian, R. A. Childs, R. D. Petrasso, V. Y. Glebov, T. C. Sangster, M. Burke, and S. Roberts, Rev. Sci. Instrum. **82**, 073502 (2011).

[19]C. K. Li, F. H. Séguin, D. G. Hicks, J. A. Frenje, K. M. Green, S. Kurebayashi, R. D. Petrasso, D. D. Meyerhofer, J. M. Soures, V. Y. Glebov, R. L. Keck, P. B. Radha, S. Roberts, W. Seka, S. Skupsky, C. Stoeckl, and T. C. Sangster, Phys. Plasmas **8**, 4902 (2001).

[20]M. G. Johnson, J. A. Frenje, R. M. Bionta, D. T. Casey, M. J. Eckart, M. P. Farrell, G. P. Grim, E. P. Hartouni, R. Hatarik, M. Hoppe, J. D. Kilkenny, C. K. Li, R. D. Petrasso, H. G. Reynolds, D. B. Sayre, M. E. Schoff, F. H. Séguin, K. Skulina, and C. B. Yeamans, Rev. Sci. Instrum. **87**, 11D816 (2016).

[21]J. A. Frenje, D. T. Casey, C. K. Li, J. R. Rygg, F. H. Séguin, R. D. Petrasso, V. Y Glebov, D. D. Meyerhofer, T. C. Sangster, S. Hatchett, S. Haan, C. Cerjan, O. Landen, M. Moran, P. Song, D. C. Wilson, and R. J. Leeper, Rev. Sci. Instrum. **79**, 10E502 (2008).

[22]M. G. Johnson, J. Katz, C. Forrest, J. A. Frenje, V. Y. Glebov, C. K. Li, R. Paguio, C. E. Parker, C. Robillard, T. C. Sangster, M. Schoff, F. H. Séguin, C. Stoeckl, and R. D. Petrasso, Rev. Sci. Instrum. **89**, 10I129 (2018).